

Estimation of Air Traffic Delay Using Three Dimensional Weather Information

Neil Y. Chen*

University of California, Santa Cruz, Moffett Field, CA 94035-1000

Banavar Sridhar†

NASA Ames Research Center, Moffett Field, CA 94035-1000

This paper describes a weather-impacted traffic index based on three-dimensional weather information and applies it to air traffic delay estimation. The weather-impacted traffic indices were generated using the high-resolution Corridor Integrated Weather System, which provides accurate, automated and high update rate information on both convective weather location and echo tops. In contrast to other methods, the new index discounts an aircraft if it can fly over the weather-impacted area safely, thus incurring no delay. The index was used as an hourly input for various National Airspace System delay estimation models. The models used traffic and weather data from June 2007 and were validated with data from July 2007. Using the index with echo tops improves the delay estimates by two percent.

I. Introduction

STUDIES show that 70% of all delays are related to weather and 60% are caused by convective weather.¹ To guide flow control decisions and identify the strategies to reduce delays, cancellations, and costs during the day of operations in various weather conditions, it is useful to create a delay estimation model and provide accurate delay estimation based on weather information.

Efforts have been made to identify the correlation between weather and delay both at the regional and national levels. The most promising concept is to use the Weather-Impacted Traffic Index (WITI), which was first introduced by Callaham et al.² Sridhar^{3,4} and Chatterji⁵ expanded the concept and built daily delay estimation models by linear regression. Klein⁶ developed objective measures of the combined impact of traffic demand and weather on the air traffic system by further combining en route WITI, terminal WITI and queuing delay to form a new metric, the National Airspace System Weather Index. Hansen⁷ developed models involving the use of econometric concepts to understand the relationship between observed airline delay and several causal factors, including traffic, airport weather, en route convective weather, and weather forecast accuracy. All of these models are two dimensional, considering only the storm location, not the echo tops. As a result, previous research in delay estimation does not take into account the ability of some aircraft to fly above echo tops.

The objective of this paper is to extend the WITI concept by adding aircraft altitude and the storm echo tops. The methodology of WITI generation in Ref. 3–5 is refined and a three dimensional WITI (3D-WITI) is generated based on data from the Corridor Integrated Weather System (CIWS).⁸ CIWS, developed and operated by MIT Lincoln Laboratory, provides both accurate precipitation and echo tops data. The relationships between CIWS WITI without echo tops information (2D-WITI), 3D-WITI, and Aviation System Performance Metrics (ASPM) delay were studied. The periodic linear models^{9,10} were used to evaluate the performance of the delay estimation.

The remainder of the paper is organized as follows. Section II provides the definition of 2D-WITI, 3D-WITI, and delay. Next, the delay estimation models are described in Section III. The delay estimation models and the methods to compute the model parameters are formulated. The results and performance of the models are demonstrated in Section IV. Finally, Section V provides conclusions.

*Research Scientist, U.C. Santa Cruz, MS 210-8.

†Senior Scientist for Air Transportation Systems, Aviation Systems Division, Fellow.

II. WITI and Delay

A. 2D-WITI

WITI is an indicator of the number of aircraft affected by weather. At given time k , the computation of WITI consists of finding: 1) the weather contours of interest $W_i(k)$, 2) the aircraft location $T_j(k)$, and 3) if aircraft $T_j(k)$ is located inside contour $W_i(k)$. It should be noted that in the second step, the aircraft location is based on the air traffic on days unaffected by weather, as described in Ref. 3–5. Considering only the projected positions of aircraft location and storm location, the 2D-WITI is formulated as follows,

$$WITI_{2D}(k) = \sum_{j=1}^{m(k)} \sum_{i=1}^{n(k)} \begin{cases} 1 & \text{if } T_j(k) \text{ is inside } W_i(k) \\ 0 & \text{if } T_j(k) \text{ is outside } W_i(k) \end{cases}, \quad (1)$$

where $n(k)$ is the number of weather contours of interest at time k , and $m(k)$ is the number of aircraft of interest at time k . The earlier WITI computations were based on the weather information provided by the National Weather Service’s Next Generation Weather Radar and the associated image processing software, referred to as NOWRAD.^{3–5}

Here CIWS is used for the WITI computation. CIWS, created by MIT Lincoln Laboratory, provides 2-hour convective forecasts updated every 5 minutes. Although the current CIWS does not cover the entire NAS, the coverage includes the major east airway and most high volume terminal areas. All or most of the Chicago Center (ZAU), New York Center (ZNY), Atlanta Center (ZTL), Houston Center (ZHU), Washington Center (ZDC), Boston Center (ZBW), Cleveland Center (ZOB), and Memphis Center (ZME) are covered by the current CIWS. The CIWS-WITI generation method has been integrated with the Future ATM Concepts Evaluation Tool (FACET).^{11,12}

Figure 1a shows a FACET display with the CIWS weather and the air traffic. The grey rectangular bounding box indicates the CIWS-covered area. The WITI computation involves finding the number of aircraft within the weather contours at a certain level, as formulated in Eq. (1). As an example, in Fig. 1b, an arbitrary level 3 contour is shown in yellow, with a total of five aircraft within the contour. Therefore, the WITI count of the contour is 5.

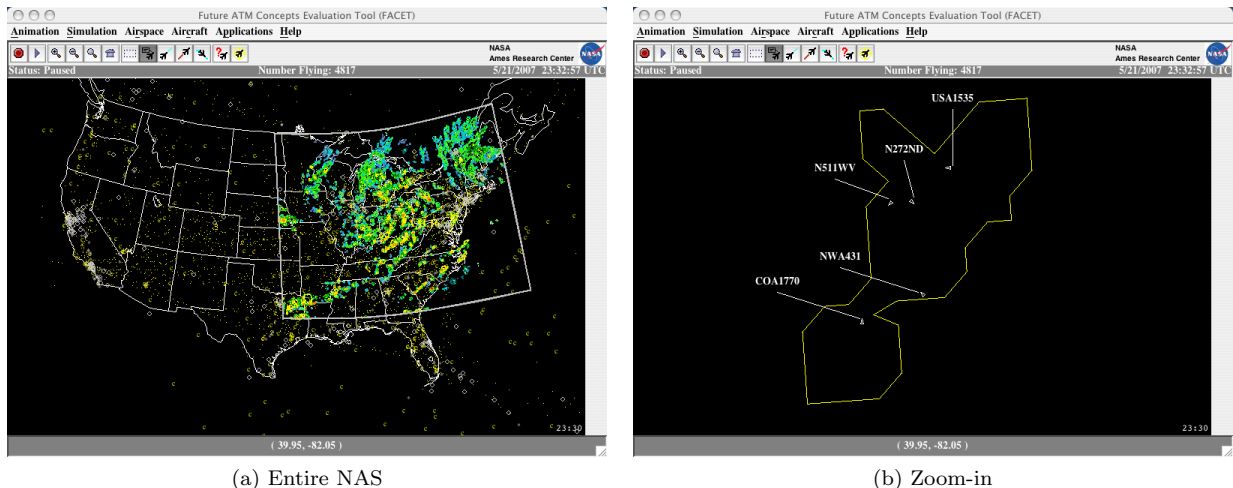


Figure 1. FACET is running with CIWS weather and air traffic loaded.

A day is defined as 24 hours starting at 0400 Eastern Standard Time (EST), since most of the aircraft departing on the previous day would have landed before 0400 (EST) and new aircraft are starting to depart after 0400 (EST). The WITI is generated at the sampling rate of 1 minute, as in previous studies.³ The CIWS data are updated every 5 minutes and are considered constant during the 5-minutes interval.

B. 3D-WITI

In addition to the precipitation weather products, CIWS provides the echo tops information, which indicates where it is safe to fly over the storms. If an aircraft is planning to fly through the area affected by the

storm but over the echo tops, it should be able to fly through the area safely, and thus is not affected by the weather. Based on this concept, the definition of WITI is extended by including the echo tops information and the altitudes of the aircraft. The echo tops products used in this study have vertical resolutions of 5,000 feet, up to 65,000 feet. Similar to the WITI defined in Eq. (1), the three dimensional WITI (3D-WITI), which considers not only the position of the aircraft but also its altitude, consists of one more element, E_i^j , which are the echo tops weather contours. The superscript i , which denotes the level of the echo tops, is defined as the vertical height divided by 5000 feet. For example, E_i^3 means the i^{th} echo tops contour is at 15,000 feet. There are 14 echo tops products available, $E_i^0 \dots E_i^{13}$. The 3D-WITI is defined as

$$WITI_{3D}(k) = \sum_{j=1}^{m(k)} \left(\sum_{i=1}^{n(k)} \begin{cases} 1 & \text{if } T_j(k) \text{ is inside } W_i(k) \\ 0 & \text{if } T_j(k) \text{ is outside } W_i(k) \end{cases} \right) \cdot \left(\sum_{i=1}^{p(k)} \begin{cases} 1 & \text{if } T_j(k) \text{ is inside } E_i^{a_j(k)}(k) \\ 0 & \text{if } T_j(k) \text{ is outside } E_i^{a_j(k)}(k) \end{cases} \right), \quad (2)$$

where $n(k)$ is the number of precipitation weather contours of interest at time k , $p(k)$ is the number of echo tops weather contours of interest at time k , $m(k)$ is the number of flying aircraft of interest at time k , and $a_j(k)$ is the altitude level defined as the aircraft altitude divided by 5000 feet rounding to the next integer. For example, if the altitude of aircraft $T_j(k)$ is 36000 feet, $a_j(k)$ is the next integer of $36000/5000 = 7.2$, which is 8.

Following the example in Fig. 1b, the echo tops at altitude level 30,000 feet in the same area are shown in Fig. 2a. There are two aircraft, indicated in yellow color, outside the echo tops contours. The aircraft flying outside the contours at the flight level over 30,000 feet means that they are flying over the storms, thus they are not affected by weather. The one in the north is at flight level 36,000 feet and the one in the south is at 34,000 feet, which means both are above the storms and should not contribute to the $WITI_{3D}$. Therefore, the $WITI_{3D}$ count for this area is 3. The three dimensional view of the CIWS echo top products is shown in Fig. 2b. It can be seen that the two yellow aircraft are above the echo tops of the storms.

Both 2D-WITI and 3D-WITI are processed using the data from June 4, 2007. Figure 3 shows a comparison between the 2D-WITI and the 3D-WITI. The time series values are shown in Fig. 3a. The hourly WITIs are defined as the sum of WITIs in every hour, and are shown in Fig. 3b. The discrepancy between the two suggests that some air traffic affected by the precipitation weather products could fly over the echo tops and would not contribute to delay in the NAS. Further analysis of the delay estimate models will be presented in the next section.

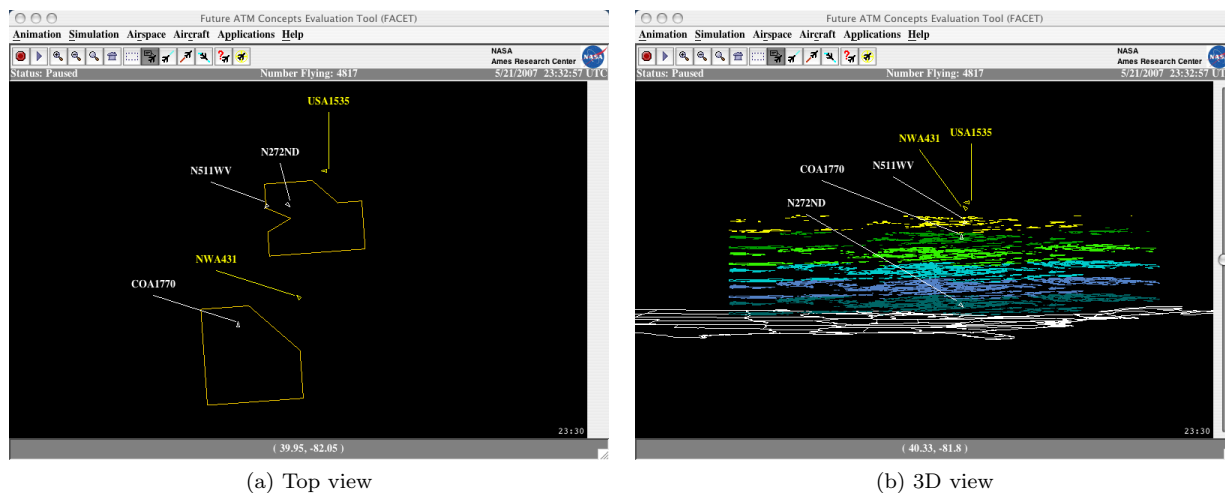
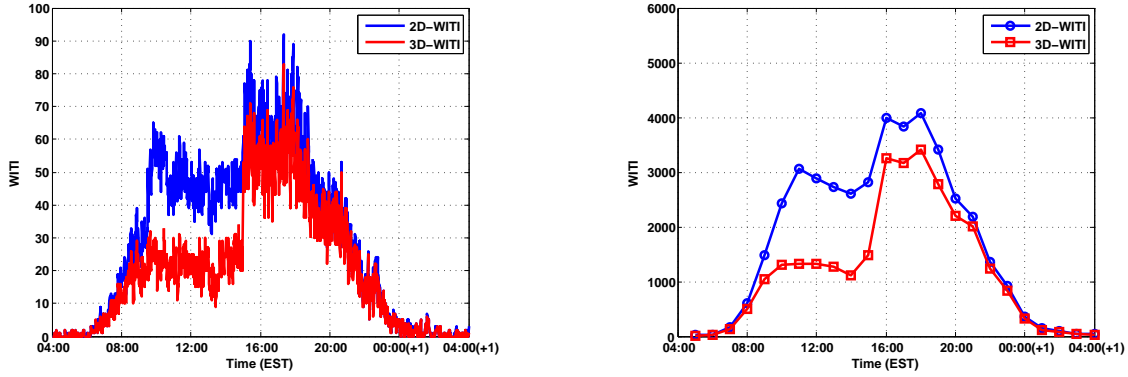


Figure 2. FACET is running with CIWS echo tops weather and air traffic loaded.

C. Delay

The air traffic delay data used in this paper are drawn from the FAA Aviation System Performance Metrics (ASPM). ASPM provides performance data at 75 domestic airports in two different sampling rates, hourly and quarter hourly. The hourly delay data are used, and only the delays at the airports covered by CIWS are considered in this paper. The 2D-WITI, 3D-WITI, and ASPM delay from June, 2007 are presented



(a) Time series

(b) Hourly

Figure 3. 2D-WITI and 3D-WITI on June 4, 2007.

in Fig. 4. As illustrated by this figure, high correlation among the three is clearly shown. Note that the ASPM delay in the figure is scaled down by $1/6$ in order to have the same level of magnitude as the WITI counts. As a reference, the monthly average correlation coefficient between 2D-WITI and ASPM delay is 0.86. There is no improvement in the monthly average correlation coefficient between 3D-WITI and ASPM over 2D-WITI. However, looking at days where there is a large discrepancy between 2D-WITI and 3D-WITI, 3D-WITI is indeed better correlated with the delay. For example, on June 4, 2007, the 2D-WITI is high at 0900(EST) while 3D-WITI remains low, as shown in Fig. 5. On June 4, the 2D-WITI and ASPM delay has a correlation coefficient of 0.84, while 3D-WITI and ASPM delay has a correlation coefficient of 0.93. This suggests even though there might be many aircraft routes covered by the bad weather, some of them should have no problem flying over the storms as planned. Thus, these aircraft should not contribute to the NAS delay, and this fact is indicated by a lack of a corresponding peak in the ASPM delay plot.

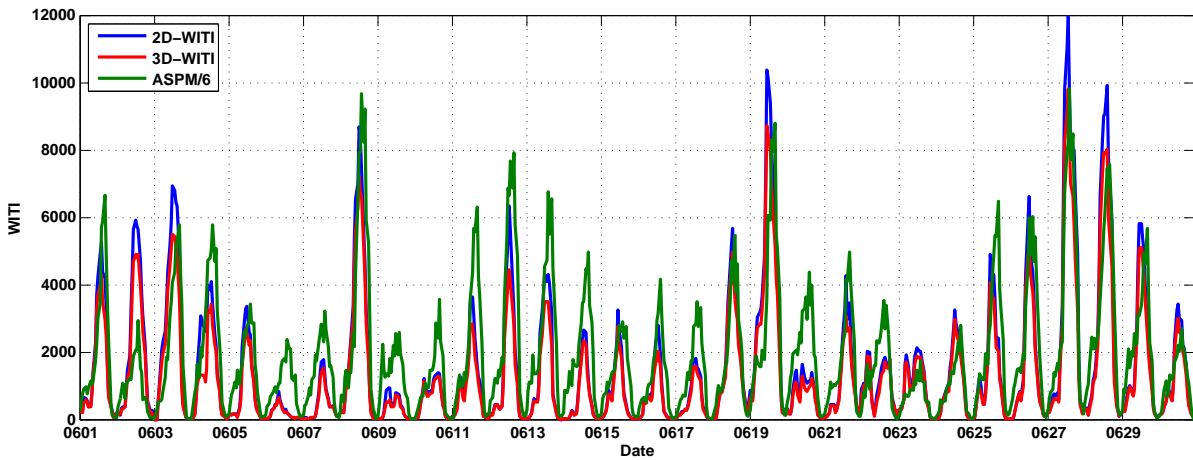


Figure 4. Hourly 2D-WITI, 3D-WITI, and ASPM delay in June, 2007

III. Delay Estimation Model

Results presented in Sridhar,^{3,4} Klein,⁶ and Hansen⁷ have shown a strong linear correlation between air traffic delay and daily WITI. We extend the research on the daily correlation and likewise find a strong linear

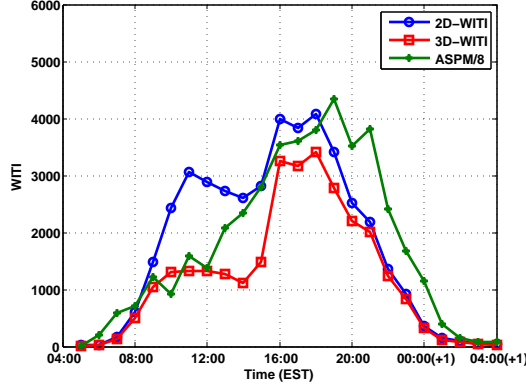


Figure 5. Hourly 2D-WITI, 3D-WITI, and ASPM delay on June 4, 2007

correlation of hourly air traffic delay with respect to hourly 2D-WITI and 3D-WITI within a day. Three classes of models are described in this section: 1) a periodic linear (PL) hourly delay model, 2) a periodic finite impulse response (PFIR) hourly delay model, and 3) a periodic linear autoregressive with exogenous inputs (PARX) hourly delay model.

A. Periodic Linear (PL) Hourly Delay Model

First, given the observed daily WITI values for p days, $\mathbf{w} = [w_1 \ w_2 \ \dots \ w_p]^T$ and the observed aggregate daily delay, $\mathbf{d} = [d_1 \ d_2 \ \dots \ d_p]^T$, the linear model for the daily delay can be formulated as

$$\mathbf{d} = \alpha \mathbf{w} + \gamma + \mathbf{e}, \quad (3)$$

where α and γ are the model coefficients and \mathbf{e} is the error estimate. The α and γ can be found by solving the least-square solution of Eq. (3). The delay estimate, $\hat{\mathbf{d}}$, can be expressed as

$$\hat{\mathbf{d}} = \alpha \mathbf{w} + \gamma, \quad (4)$$

Next, as seen in Fig. 4, both the ASPM delay and WITI have a 24-hour period. Instead of using the aggregate daily delay and WITI, the hourly data can be used to build the delay model. The daily delay model can be divided into 24 individual hourly delay models. Given the observed hourly WITI and delay on p days, the WITI and delay data matrices are defined as

$$W = \begin{bmatrix} w_{1,1} & w_{2,1} & \dots & w_{24,1} \\ \vdots & \vdots & \ddots & \vdots \\ w_{1,p} & w_{2,p} & \dots & w_{24,p} \end{bmatrix}, \quad D = \begin{bmatrix} d_{1,1} & d_{2,1} & \dots & d_{24,1} \\ \vdots & \vdots & \ddots & \vdots \\ d_{1,p} & d_{2,p} & \dots & d_{24,p} \end{bmatrix}, \quad (5)$$

where $w_{i,j}$ and $d_{i,j}$ are the hourly WITI and delay at hour i on day j . Assume \mathbf{w}_h and \mathbf{d}_h are the h^{th} columns of W and D , which represent the hourly WITI and delay at hour h of the observed days. Note that $h = 1, 2, \dots, 24$, and it starts at 0400(EST). The delay model at hour h is described as

$$\mathbf{d}_h = \alpha_h \mathbf{w}_h + \gamma_h + \mathbf{e}_h, \quad (6)$$

where α 's and γ 's can be found by solving the least-square solution of Eq. (6). The estimate of the hourly delay $\hat{\mathbf{d}}_h$ can then be expressed as

$$\hat{\mathbf{d}}_h = \alpha_h \mathbf{w}_h + \gamma_h. \quad (7)$$

The model in Eq. (6) and Eq. (7) is referred to as the periodic linear hourly delay model.

B. Periodic Finite Impulse Response (PFIR) Hourly Delay Model

The periodic linear delay model considers only the relationship between current delay and current WITI. In reality, the delay might be caused by not only the current weather but also the weather hours earlier. Assuming the current delay is correlated with the current WITI and the WITI in the previous hour, the model can be described as

$$\mathbf{d}_h = \alpha_{h,0} \mathbf{w}_h + \alpha_{h,1} \mathbf{w}_{h-1} + \gamma_h + \mathbf{e}_h. \quad (8)$$

The α 's and γ 's can be found by solving the least-square solution of Eq. (8). The estimate of hourly delay $\hat{\mathbf{d}}_h$ can be formulated as

$$\hat{\mathbf{d}}_h = \alpha_{h,0} \mathbf{w}_h + \alpha_{h,1} \mathbf{w}_{h-1} + \gamma_h. \quad (9)$$

The model in Eq. (8) and Eq. (9) is referred to as the first-order PFIR model with direct feed-through. First-order means that data one time-step earlier was used and the direct feed-through means that current data are used to build the model.

More generally, the n^{th} -order PFIR model can be formulated as

$$\mathbf{d}_h = \sum_{k=0}^n \alpha_{h,k} \mathbf{w}_{h-k} + \gamma_h + \mathbf{e}_h, \quad (10)$$

$$\hat{\mathbf{d}}_h = \sum_{k=0}^n \alpha_{h,k} \mathbf{w}_{h-k} + \gamma_h. \quad (11)$$

Note that \mathbf{w}_{h-k} is defined as $\mathbf{0}$ for $h \leq k$, which implies that the least-square solutions of $\alpha_{h,k}$ are 0's for $h \leq k$. Also, the PL model described in the previous subsection is a special case of the PFIR model when $n = 0$.

C. Periodic Linear Autoregressive with Exogenous Inputs (PARX) Hourly Delay Model

At a given hour h , in addition to the current and past WITI, the past delay might also be available in certain applications such as real-time delay prediction.¹³ Assuming the current delay is correlated with the current WITI, the WITI in the past n hours, and the delay in the past m hours, the model can be formulated as

$$\mathbf{d}_h = \sum_{k=0}^n \alpha_{h,k} \mathbf{w}_{h-k} + \sum_{l=1}^m \beta_{h,k} \mathbf{d}_{h-l} + \gamma_h + \mathbf{e}_h, \quad (12)$$

$$\hat{\mathbf{d}}_h = \sum_{k=0}^n \alpha_{h,k} \mathbf{w}_{h-k} + \sum_{l=1}^m \beta_{h,k} \mathbf{d}_{h-l} + \gamma_h, \quad (13)$$

where α 's, β 's, and γ 's can be found by solving the least-square solution of Eq. (12). This model is referred to as the PARX model with order (n, m) . Note that the PFIR model in the previous subsection is a subset of PARX model when $m = 0$.

To be more explicit, Eq. (12) can be rewritten as

$$\mathbf{d}_h = \begin{bmatrix} \mathbf{w}_h & \dots & \mathbf{w}_{h-n} & \mathbf{d}_{h-1} & \dots & \mathbf{d}_{h-m} & 1 \end{bmatrix} \begin{bmatrix} \alpha_{h,0} \\ \vdots \\ \alpha_{h,n} \\ \beta_{h,1} \\ \vdots \\ \beta_{h,m} \\ \gamma_h \end{bmatrix} + \mathbf{e}_h. \quad (14)$$

The Moore-Penrose pseudo-inverse¹⁴ is used to solve the equation. The solution is described as

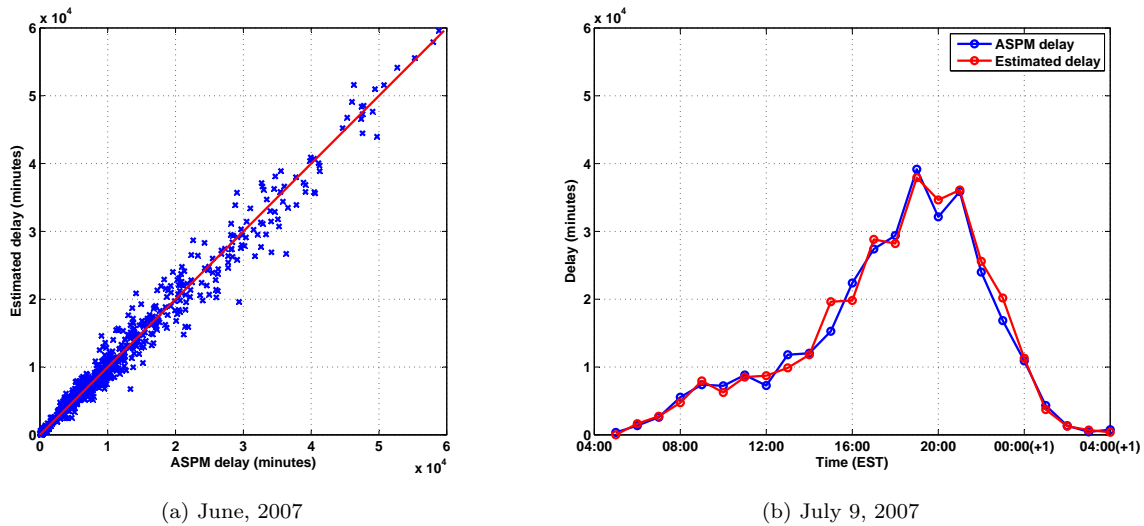
$$\begin{bmatrix} \alpha_{h,0} & \dots & \alpha_{h,n} & \beta_{h,1} & \dots & \beta_{h,m} & \gamma_h \end{bmatrix}^T = \begin{bmatrix} \mathbf{w}_h & \dots & \mathbf{w}_{h-n} & \mathbf{d}_{h-1} & \dots & \mathbf{d}_{h-m} & 1 \end{bmatrix}^\dagger \mathbf{d}_h, \quad (15)$$

where $[\cdot]^\dagger$ represents the pseudo-inverse of the matrix.

IV. Results

The delay and 3D-WITI data for the month of June, 2007 were used as reference data to build a PARX model, described in Eq. (12), with model order $(n, m) = (1, 1)$. In this model, there are a total of 96 model parameters to be identified, including $\alpha_{1,0} \dots \alpha_{24,0}$, $\alpha_{1,1} \dots \alpha_{24,1}$, $\beta_{1,1} \dots \beta_{24,1}$, and $\gamma_1 \dots \gamma_{24}$. Once the parameters are identified, Eq. (13) is used to compute the estimate of the hourly delay on reference days, $\hat{\mathbf{d}}_h$. Figure 6a shows the actual ASPM hourly delay \mathbf{d}_h versus the estimate of the hourly delay $\hat{\mathbf{d}}_h$ on all the reference days. The red line in the figure indicates the perfect estimates. As shown in the figure, all the dots lie around the red line which suggests \mathbf{d}_h and $\hat{\mathbf{d}}_h$ are close. The average daily root-mean-square (RMS) error between \mathbf{d}_h and $\hat{\mathbf{d}}_h$, or \mathbf{e}_h , is 1714 minutes, which yields only 5.83% of the average RMS of daily ASPM delay in June, 2007, which is 29403 minutes.

Next, a day not in the reference days was selected to evaluate the performance of the delay estimation model. For July 9, 2007, which has total ASPM delay of 324577 minutes, Fig. 6b shows the actual ASPM delay and the estimated delay. The RMS error between the actual ASPM delay and the delay estimate is 1573 minutes, only 5.54% of the RMS of the actual ASPM delay.



(a) June, 2007 (b) July 9, 2007

Figure 6. ASPM delay and estimated delay

Furthermore, the PARX models with different order (n, m) were used to evaluate the performance of air traffic delay estimates using 2D-WITI and 3D-WITI. The pair (n, m) is the order of the model, where n is the number of past WITI and m is the number of past delay used in the model. There are different variations of the models. For example, for $m = 0$, the delay estimates are related to the WITI and do not depend on past values of delay. These models are essentially PFIR models, and $n = 0$ represents the simple PL model. On the other hand, for $n = 0$, the delay estimates are only related to the past delays and do not depend on the WITI. The models are periodic autoregressive (PAR) models. The PAR models are used as the baseline to evaluate how much improvement can be achieved with the WITI information. The whole month of data from July, 2007 are used to validate the models. All PL, PFIR, PAR and PARX models using both 2D-WITI and 3D-WITI with different orders were tested.

The results are summarized in Table 1 and 2. As shown in Table 1, the PFIR models do not perform well because of the lack of past delay information. In Table 2, it shows that the PARX model with order $(1, 1)$ using 3D-WITI is slightly better than the other models. It was noticed that higher order models do not provide better performance for this class of models. The reason might be higher order models tend to over fit the observed data and lose the generality for the validation data. The PARX model using 3D-WITI with order $(1, 1)$ was selected as the best for this class of models. In this case, the average daily RMS error of the model is 1876 minutes, mean absolute error is 1382 minutes, and maximum error is 4762 minutes. It provides a small improvement (about 2%) in delay estimation over other methods. Figure 7 shows the correlation between the actual delay and the optimal estimated delay for each hour in July, 2007. The correlation coefficient between the two is 0.98.

Table 1. Validation for the PFIR models with different parameters using July, 2007 data. The numbers are in minutes.

Model	2D PL	2D PFIR		3D PL	3D PFIR	
(n,m)	(0,0)	(1,0)	(2,0)	(0,0)	(1,0)	(2,0)
RMS error	4791	4801	4850	4814	4784	4907
Mean absolute error	3602	3567	3692	3629	3570	3761
Maximum error	10861	11011	10830	10940	11050	10971

Table 2. Validation for the PARX models with different parameters using July, 2007 data. The numbers are in minutes.

Model	PAR		2D PARX		3D PARX	
(n,m)	(0,1)	(0,2)	(1,1)	(2,2)	(1,1)	(2,2)
RMS error	1920	2050	1895	2086	1876	2070
Mean absolute error	1388	1496	1399	1525	1382	1513
Maximum error	5074	5273	4800	5433	4762	5433

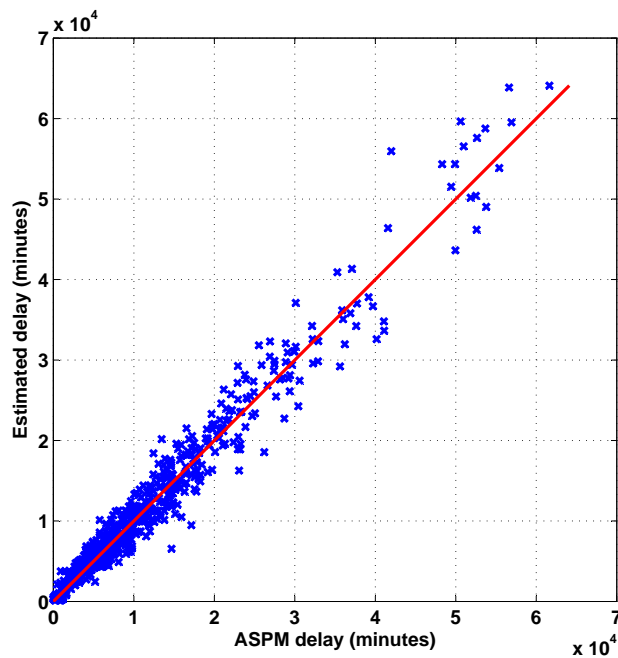


Figure 7. Hourly ASPM delay and estimated delay in July, 2007.

V. Conclusions and Future Work

In this paper, a new three-dimensional weather-impacted traffic index was developed and presented. The new index uses the aircraft altitude and the storm echo tops information to discount an aircraft if it can fly over the weather-impacted area safely, thus incurring no delay. Both 2D-WITI and 3D-WITI were computed using CIWS weather product, which provides both accurate precipitation and echo tops weather information. The delay estimation methodology utilizes the hourly resolution of the ASPM data. The indices were used as exogenous inputs for periodic autoregressive models to perform the NAS delay estimation. Various linear hourly models using different combinations of past and current weather and traffic information were examined to determine the optimal delay estimation model. The models were built using traffic and weather data from June 2007, and were validated with the data from July 2007. The recursive models using WITI information outperform models using only delay information. Another result from the study is that using higher order models may not provide more accurate estimates due to overfitting of the data. No clear conclusions can be drawn about the additional benefits of using 3D-WITI information versus 2D-WITI information.

The performance of 3D-WITI models need more examination. The result shows that the 3D-WITI provides a small improvement (about 2%) in delay estimation. The reason that using 3D-WITI does not provides significant superior performance over using 2D-WITI might be that the aircraft do not take full advantage of the echo tops information to fly over storm. Further studies, with larger datasets and a better understanding of how echo top information is used by pilots and air traffic controllers may lead to more accurate delay estimates. Accurate delay estimates will benefit the ATM in identifying the strategies to reduce delays, cancelations, and costs during operations in severe weather conditions.

References

- ¹National Research Council, *Weather Forecasting Accuracy for FAA Traffic Flow Management*, The National Academies Press, Washington, DC, 2003.
- ²Callahan, M. B., DeArmon, J. S., Cooper, A., Goodfriend, J. H., Moch-Mooney, D., and Solomos, G., "Assessing NAS Performance: Normalizing for the Effects of Weather," *4th USA/Europe Air Traffic Management R&D Symposium*, Santa Fe, NM, December 2001.
- ³Sridhar, B. and Swei, S., "Relationship between Weather, Traffic and Delay Based on Empirical Methods," *6th AIAA Aviation Technology, Integration and Operations Conference (ATIO)*, Wichita, KS, September 2006.
- ⁴Sridhar, B. and Swei, S., "Classification and Computation of Aggregate Delay Using Center-Based Weather Impacted Traffic Index," *7th AIAA Aviation Technology, Integration and Operations Conference (ATIO)*, Belfast, Northern Ireland, September 2007.
- ⁵Chatterji, G. and Sridhar, B., "National Airspace System Delay Estimation Using Weather Weighted Traffic Counts," *AIAA Guidance, Navigation and Control Conference*, San Francisco, CA, August 2005.
- ⁶Klein, A., Jehlen, R., and Liang, D., "Weather Index With Queuing Component For National Airspace System Performance Assessment," *7th USA-Europe ATM R&D Seminar*, Barcelona, Spain, July 2007.
- ⁷Hansen, M. and Xiong, J., "Weather Normalization for Evaluating National Airspace System (NAS) Performance," *7th USA-Europe ATM R&D Seminar*, Barcelona, Spain, July 2007.
- ⁸Evans, J. and Klinge-Wilson, D., "Description of the Corridor Integrated Weather System (CIWS) Weather Products," Project Report ATC-317, MIT Lincoln Laboratory, August 2005.
- ⁹Ljung, L., *System Identification: Theory for the User*, Prentice Hall, Englewood Cliffs, NJ, 2nd ed., 1999.
- ¹⁰Franses, P. and Papp, R., *Periodic Time Series Models*, Oxford Univ. Press, London, UK, 2003.
- ¹¹Bilimoria, K., Sridhar, B., Chatterji, G. B., Sheth, K., and Grabbe, S., "FACET: Future ATM Concepts Evaluation Tool," *Air Traffic Control Quarterly*, Vol. 9, No. 1, 2001, pp. 1–20.
- ¹²Sridhar, B., Sheth, K., Smith, P., and Leber, W., "Migration of FACET from Simulation Environment to Dispatcher Decision Support System," *24th Digital Avionics Systems Conference*, Vol. 1, November 2005, pp. 3.E.4–31–12.
- ¹³Sridhar, B. and Chen, N., "Short Term National Airspace System Delay Prediction Using Weather Impacted Traffic Index," *AIAA Guidance, Navigation and Control Conference*, Honolulu, HI, August 2008, to appear.
- ¹⁴Golub, G. H. and Van Loan, C. F., *Matrix Computations*, The Johns Hopkins University Press, Baltimore, MD, 3rd ed., 1996.